An Improved Understanding for the Transient Operation of the Power Insulated Gate Bipolar Transistor (IGBT)*

ALLEN R. HEFNER, JR., MEMBER, IEEE

Abstract—It is shown that a non-quasi-static analysis must be used to describe the transient current and voltage waveforms of the IGBT. The non-quasi-static analysis is necessary because the transport of electrons and holes are coupled for the low-gain, high-level injection conditions, and because the quasi-neutral base width changes faster than the base transit speed for typical load circuit conditions. To verify that both of these non-quasi-static effects must be included, the predictions of the quasi-static and non-quasi-static models are compared with measured current and voltage switching waveforms. The comparisons are performed for different load circuit conditions and for different device base lifetimes.

I. INTRODUCTION

THE insulated gate bipolar transistor (IGBT) is a new power device with an insulated gate input like that of a power MOSFET but with the low on-state resistance of a power bipolar transistor [1], [2]. A schematic of the structure of two of the many thousands of cells of an n-channel IGBT is shown in Fig. 1. The IGBT functions as a bipolar transistor that is supplied based current by the drain of a MOSFET where the source of the MOSFET is shorted to the collector of the bipolar transistor (Fig. 2), [3]. The regions of each of these components are labeled on the right half of Fig. 1. The bipolar transistor of the IGBT consists of a lightly doped wide base with the base virtual contact (MOSFET drains) near the collector end of the base. This bipolar transistor has a low gain and is in the high-level injection condition for the practical current density range of the IGBT.

Several analytical models have been proposed to describe the operating characteristics of the IGBT [4]-[11]. Each model uses ambipolar transport theory to describe the transport of electrons and holes in the base, but there are significant differences between the models in the approach taken to describe the transient operation. The major difference between the models proposed by Fossum *et al.* [10], [11] and Kuo *et al.* [9], and that proposed by
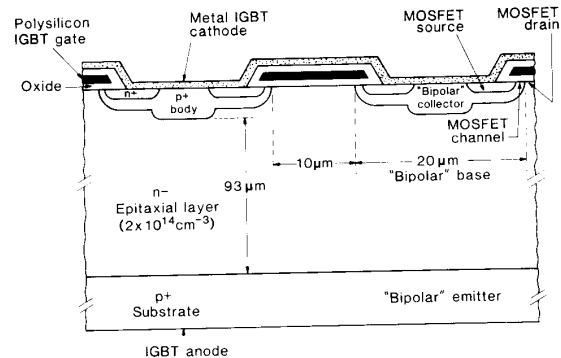
Fig. 1. Diagram of two diffused cells of n-channel IGBT. Device consists of many thousands of these cells which in effect operate in parallel.
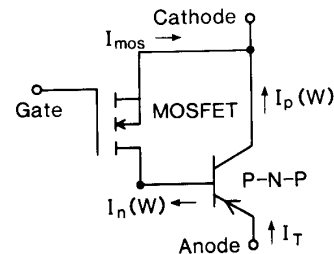

Fig. 2. Equivalent circuit model of IGBT.

Hefner [4]-[8] is that the former models assume the quasi-static (QS) condition for the transient analysis and the latter model was derived using a non-quasi-static (NQS) analysis. Recently though, Fossum *et al.* [12] have included NQS effects to describe the IGBT.

It is well known that the QS approximation is not valid for bipolar transistors at high speeds because a finite base transit time is required for a change in injected base charge to traverse the base and appear as a change in collector current [13], [14]. Although the base charge does not change rapidly for the IGBT, it is shown in this paper that the QS approximation is not valid for the IGBT and other conductivity-modulated devices. The QS approximation is not valid for the IGBT because: 1) the transport of electrons and holes are coupled for the low-gain, high-level injection conditions [4]-[8], and 2) the quasi-neutral base

width changes faster than the base transient speed for typical loading conditions [6]–[8]. It is also shown that these NQS effects are only important for the low-gain, high-level injection conditions of conductivity-modulated power devices such as the IGBT but are unimportant for typical operation of signal transistors.

II. IGBT DEVICE PHYSICS

The analysis of the bipolar transistor portion of the IGBT is described using the coordinate system defined in Fig. 3 and the symbols defined in the Nomenclature section. The collector-base junction of the bipolar transistor of the IGBT is reverse biased for forward conduction and the depletion region of the collector-base junction extends into the base. The collector-base junction depletion width is given by

$$W_{bcj} = \sqrt{\frac{2\epsilon_{si}(V_{bc} + V_{bi})}{qN_B}},\qquad (1a)$$

and the width of the quasi-neutral base is given by

$$W = W_B - W_{bcj} \qquad (1b)$$

where $V_{bi} \approx 0.7$ V. The effect of mobile carriers on the depletion layer space charge concentration is accounted for as described in [6]–[8].

Because of the IGBT structure (Fig. 1), the bipolar transistor base current (electrons) supplied by the MOSFET is introduced at the collector end of the base. In the model, the region of the device at the epitaxial layer edge of the reverse-biased epitaxial layer-body junction ($x = W$) is designated as the contact between the bipolar transistor base and the MOSFET drain. The electron current that enters this region $I_n(W)$ is the bipolar transistor base current which is supplied by the MOSFET drain, and the hole current there $I_p(W)$ is the collector current of the bipolar transistor (see Fig. 2).

Because the base of the bipolar transistor of the IGBT is in the high-level injection condition for the practical current density range of the device, $n \approx p$, and the transport of electrons and holes in the base are described by the ambipolar transport equations [15]:

$$I_n = \frac{b}{1 + b} I_T + qAD \frac{\partial p}{\partial x} \qquad (2)$$

$$I_p = \frac{1}{1 + b} I_T - qAD \frac{\partial p}{\partial x}. \qquad (3)$$

Notice that the transport of electrons and holes are coupled by the total current, I_T, so they cannot be treated independently. This is important for the bipolar transistor of the IGBT because the gain is low and the electron and hole currents are of comparable magnitude. This coupling results in NQS operation for the IGBT because the flow of electrons from the collector end of the base toward the emitter interacts with the flow of holes from the emitter toward the collector end of the base. This coupling is very weak for high-gain or low-level injection conditions [6],
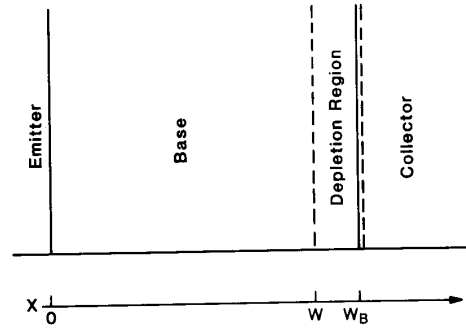

Fig. 3. Coordinate system used to develop IGBT bipolar transistor model. Emitter, base, and collector regions correspond to those indicated on right half of Fig. 1.

[7], so this NQS effect is only important for the low-gain, high-level injection conditions of conductivity-modulated power devices.

The time-dependent ambipolar diffusion equation is given by

$$\frac{\partial^2 \delta p}{\partial x^2} = \frac{\delta p}{L^2} + \frac{1}{D} \frac{\partial \delta p}{\partial t}, \qquad (4)$$

and is valid for devices in which I_T is independent of position such as the IGBT where the base current is introduced at the collector end of the base. This equation is solved for the boundary conditions and initial condition to determine the distribution of excess carriers in the base. This distribution is then used in (2) and (3) to determine the currents. The boundary condition for the excess carrier concentration at the emitter edge of the quasi-neutral base ($x = 0$) is

$$\delta p(x = 0) \equiv P_0 \qquad (5a)$$

where P_0 is used as a parameter for the development of the model, and at the collector edge of the quasi-neutral base ($x = W$), the boundary condition is

$$\delta p(x = W) = 0 \qquad (5b)$$

because the collector-base junction is reverse biased for forward operation of the IGBT (anode positive).

For the voltage transitions of typical IGBT transient operation, the quasi-neutral base width (W of (5b)) changes in a time on the order of the base transit time and the solution to (4) must account for the moving boundary condition. From (1), the time rate of change of quasi-neutral base width is given in terms of the time rate of change of collector-base voltage by

$$\frac{dW}{dt} = \frac{-C_{bcj}}{qN_B A} \cdot \frac{dV_{bc}}{dt}, \qquad (5c)$$

where $C_{bcj} \equiv A\epsilon_{si}/W_{bcj}$ is the instantaneous value of collector-base depletion capacitance. This moving quasi-neutral base width boundary condition results in an additional component of NQS collector current. This compo-

nent of current is larger than the displacement current through the collector-base junction depletion-capacitance for the high-level injection condition, and is a significant component of the total collector current for the low-gain condition. This NQS effect is unimportant, though, for the low-level injection or high-gain conditions of signal transistors.

III. TRANSIENT MODELING

It is assumed in the QS approach that the collector current during the transient is determined exclusively by the instantaneous base charge and terminal voltages using the steady-state relationships. However, for the bipolar transistor of the IGBT, the collector current during the transient also depends upon: 1) the instantaneous total current because the transport of electrons and holes are coupled, and upon 2) the time rate of change of the quasi-neutral base width because it changes faster than the base transit speed. In this section, both a QS model and an NQS model are presented.

Quasi-Static Analysis

In this subsection, expressions are presented for the steady-state excess carrier distribution in the base of the bipolar transistor of the IGBT and for the steady-state collector and base currents. It is assumed in the QS approach that the steady-state expressions are also valid for transient conditions. The steady-state expressions developed in this subsection are used below by the QS model to describe the transient current and voltage waveforms, and are also used as initial conditions for the NQS transient model.

The solution to the steady-state ambipolar diffusion equation ((4) with $\partial \delta p / \partial t = 0$) for the steady-state boundary conditions ((5) for $dW/dt = 0$) is

$$\delta p(x) = P_0 \frac{\sinh\left(\dfrac{W - x}{L}\right)}{\sinh\left(\dfrac{W}{L}\right)}, \tag{6}$$

where P_0 is used as a parameter for the development of the model. The total excess carrier base charge Q is obtained in terms of P_0 by integrating this carrier distribution through the base:

$$Q = qP_0AL \tanh \frac{W}{2L}. \tag{7}$$

This charge is used as an initial condition for the transient analysis, and this expression is used by the QS transient analysis to relate the instantaneous values of Q and P_0.

Using the quasi-equilibrium approximation for the high-level injection condition, the electron current injected into the emitter is given by

$$I_n(x = 0) = I_{sne} \frac{P_0^2}{n_i^2}, \tag{8}$$

where I_{sne} is the emitter electron saturation current. The steady-state base current $I_n(x = W)$ and collector current $I_p(x = W)$ are then obtained from (2), (3), (6), and (8):

$$I_n(W) = \frac{P_0^2 I_{sne}}{n_i^2} + \frac{qP_0AD}{L}\left(\coth\left(\frac{W}{L}\right) - \frac{1}{\sinh\left(\dfrac{W}{L}\right)}\right) \tag{9}$$

$$I_p(W) = \frac{P_0^2 I_{sne}}{bn_i^2} + \frac{qP_0AD}{L}\left(\frac{\coth\left(\dfrac{W}{L}\right)}{b} + \frac{1}{\sinh\left(\dfrac{W}{L}\right)}\right). \tag{10}$$

These steady-state currents are related to the charge Q by substituting the expression for P_0 obtained from (7) into (9) and (10). It is assumed in the QS approach that this steady-state relationship between the collector current and the charge is also valid for transient conditions. In Section IV, it is shown how these steady-state expressions are used in the QS approach to describe the transient current and voltage waveforms.

Non-Quasi-Static Analysis

In this subsection, expressions are presented for the NQS transient excess carrier distribution and collector current. These expressions differ from those for the QS model in that they depend upon: 1) the instantaneous total current and upon 2) the time rate of change of the quasi-neutral base width. It is shown in the next section how these expressions are used to describe the transient current and voltage waveforms and that the NQS effects dominate IGBT transient operation.

Because the quasi-neutral base width changes with the changing collector-base voltage, (5c), the excess carrier base charge Q is swept into a quasi-neutral base that becomes narrower as the voltage is increased. This is illustrated in Fig. 4(a) for a simplified excess carrier distribution where the change in local excess carrier concentration Δp that results throughout the base for a change in base width ΔW is indicated. For comparison, Fig. 4(b) shows the change in local excess carrier concentration that results for a change in total base charge ΔQ which is important for high-speed operation of signal transistors [13]. It is clear from Fig. 4(a) that the time rate of change of local excess carrier concentration $\partial \delta p / \partial t$ depends upon the quasi-neutral base width boundary velocity dW/dt. Therefore, because $\partial \delta p / \partial t$ appears in the second term on the right-hand side of (4), a curvature in the carrier distribution given by the left-hand side of (4) is required to bring about the redistribution of carriers for the moving boundary condition.

Thus, in general, (4) must be solved for the conditions of a moving boundary to describe the NQS transient carrier distribution and collector current. A first-order solution to (4) for the moving quasi-neutral base width bound-
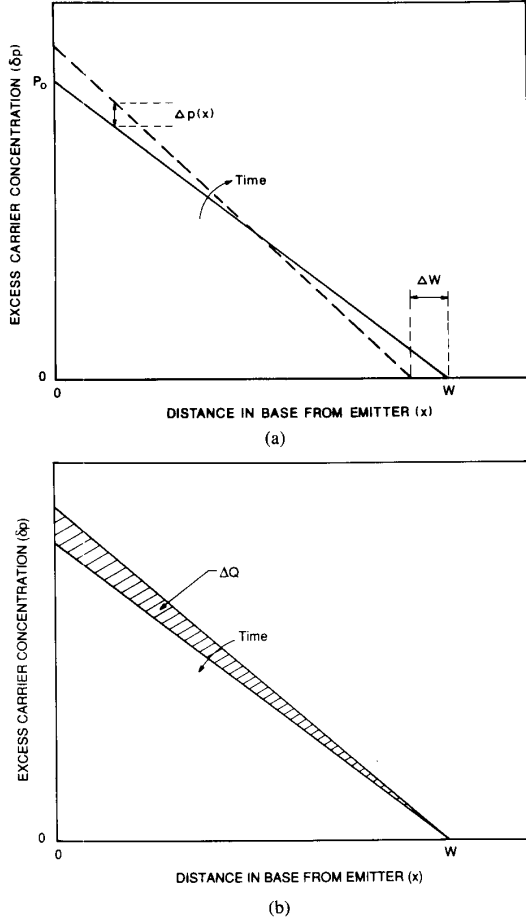
(a)

(b)

Fig. 4. (a) Simplified excess carrier distribution in base indicating change in local excess carrier concentration with time due to moving quasi-neutral base width boundary. (b) Simplified excess carrier distribution in base indicating change in local excess carrier concentration due to change in total base charge.

ary condition is given by [6]–[8]:

$$\delta p'(x) = P_0' \left[1 - \frac{x}{W'} \right]$$

$$- \frac{P_0'}{W'D} \left[\frac{x^2}{2} - \frac{W'x}{6} - \frac{x^3}{3W'} \right] \cdot \frac{dW'}{dt}, \quad (11)$$

where parameters that change with time are distinguished with a prime for the NQS transient analysis. This carrier distribution is shown in Fig. 5 and consists of a linear component (first term) and a moving boundary redistribution component (second term). For a constant anode voltage, only the first term on the right-hand side of (11) remains. The first term differs from the steady-state carrier distribution because the electrons and holes that recombine in the base are no longer supplied by the divergence of their current densities as they are in steady state, but are only supplied by (and thus reduce) the local excess carrier concentration (i.e., the left-hand side of (4) becomes zero). The second term on the right-hand side of
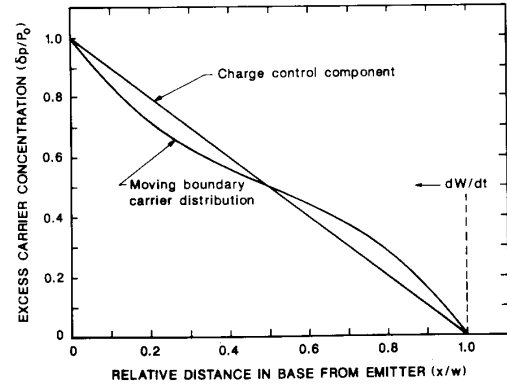

Fig. 5. Excess carrier distribution in base for given quasi-neutral base width boundary velocity.

(11) provides the curvature in the carrier distribution necessary to redistribute the excess carriers for a given quasi-neutral base width boundary velocity dW/dt.

By integrating (11) through the base, the total base charge is given in terms of P_0 for the transient conditions by

$$Q' = \frac{qP_0'AW'}{2}. \quad (12)$$

The NQS transient collector current is then obtained by evaluating (3) at $x = W$ using the NQS carrier distribution of (11):

$$I_p'(W') = \left(\frac{1}{1+b} \right) I_T' + \left(\frac{b}{1+b} \right) \frac{4D_p}{W'^2} Q'$$

$$- \frac{Q'}{3W'} \cdot \frac{dW'}{dt}, \quad (13)$$

where the Einstein relations, $D_{n,p} = (kT/q) \mu_{n,p}$, and the expressions for b and D in the Nomenclature section have been used. The first term on the right-hand side of (13) is an NQS term that shows the explicit dependence of the collector current upon the instantaneous total current due to the coupling between the transport of electrons and holes. The second term is a charge-control component of current (I_{CC}) because it is directly related to the charge that remains in the base and to the applied collector-base voltage using (1). The third term is necessary to bring about the redistribution of carriers for the moving quasi-neutral base width boundary condition. This moving boundary redistribution component of current (I_R) is an NQS component because it depends upon the time rate of change of base width in addition to the instantaneous value of base width.

The NQS expression for collector current, (13), differs substantially from the QS expression, (10), in that it depends upon: 1) the instantaneous total current and 2) the time of change of the quasi-neutral base width. The explicit dependence upon the total current is important for the low-gain condition where the base current $I_n(W)$ is a

significant component of the total current I_T, so that the collector current $I_p(W)$ is significantly affected by changes in instantaneous base current. Otherwise, for a high-gain condition, the total current is approximately equal to the collector current and the first term can be combined with the left-hand side of (13) resulting in the usual expression for the high-gain, high-level injection charge control component of collector current ($I_p(W) = 4D_pQ/W^2$). The physical significance of the redistribution component of current is ascertained by dividing the third term of (13), I_R, by the second term, I_{CC}:

$$\frac{I_R}{I_{CC}} = \left(\frac{1 + \frac{1}{b}}{3}\right) \cdot \frac{\tau_b'}{W'} \cdot \frac{dW'}{dt}, \tag{14}$$

where $\tau_b \equiv W^2/4D_p$ is the high-gain, high-level injection base transit time. This indicates that the redistribution component of current becomes comparable to the charge control component when the base width changes as fast as the base transit speed W/τ_b.

IV. IGBT TRANSIENT OPERATION

In this section, it is shown how the QS and NQS models presented above are used to derive state equations for the IGBT turn-off transient with a rapid gate voltage transition. Using these state equations, it is also shown that the NQS effects described above dominate the IGBT transient operation for the low-gain, high-level injection condition.

To turn off the IGBT, the gate voltage is switched below threshold, which rapidly removes the MOSFET channel current and eliminates the base current to the bipolar transistor. The bipolar transistor collector current falls more slowly though, since the stored excess carriers in the now open base bipolar transistor must decay. For simplicity, the simulations and measurements of this work are made for rapid gate-voltage transitions so that the MOSFET portion of the device is turned off rapidly and the MOSFET current is zero during the transient.

For this case of zero MOSFET current during the transient, the electron current at the collector edge of the quasi-neutral base ($x = W$) is equal to the displacement current through the collector-base junction depletion capacitance: $I_n(x = W) = C_{bcj} \cdot dV_{bc}/dt$. Then, because the total current at $x = W$ is the sum of the hole and electron components,

$$C_{bcj}' \frac{dV_{bc}'}{dt} = I_T' - I_p'(W'). \tag{15}$$

Also, for the case of zero MOSFET current during the transient, the excess carrier base charge decays by recombination in the base and by electron current injection into the emitter, given by (8):

$$\frac{dQ'}{dt} = -\frac{Q'}{\tau_{HL}} - I_{sne}\frac{P_0'^2}{n_i^2}, \tag{16}$$

where the collector-base depletion capacitance displacement current is negligible.

The right-hand sides of (15) and (16) are evaluated using (7) and (10) for the QS model, or (12) and (13) for the NQS model to obtain expressions for dV_{bc}/dt and dQ/dt in terms of the instantaneous valuses of I_T, Q, and V_{bc}, where W and C_{bcj} are given in terms of the instantaneous valuse of collector-base voltage using (1). The current I_T is expressed in terms of the state variables of the load circuit, so these expressions constitute a set of state equations for the IGBT where Q and V_{bc} are the state variables. To describe the IGBT transient current and voltage waveforms, the IGBT state equations are integrated simultaneously with the state equations of the load circuit using the initial conditions from the steady-state analysis. For the high-voltage transients discussed in this paper, the anode voltage V_A is assumed to be equal to V_{bc}. Also, the effect of mobile carriers on the depletion layer space charge concentration is accounted for as described in [6]–[8].

Quasi-Static State Equations

The QS voltage state equation is obtained by substituting the QS collector current, (10), into the right-hand side of (15), and by then using the QS expression for P_0 in terms of Q obtained from (7). The QS charge state equation is obtained by substituting the QS expression for P_0 in terms of Q obtained from (7) into (16). The resulting QS state equations are given by

$$\frac{dV_{bc}}{dt} = \frac{1}{C_{bcj}}\left[I_T - \frac{Q^2 I_{sne}}{b\left(n_i qAL \tanh\frac{W}{2L}\right)^2}\right.$$
$$\left. - \frac{QD}{L^2 \tanh\frac{W}{2L}}\left(\frac{\coth\left(\frac{W}{L}\right)}{b} + \frac{1}{\sinh\left(\frac{W}{L}\right)}\right)\right] \tag{17}$$

$$\frac{dQ}{dt} = -\frac{Q}{\tau_{HL}} - I_{sne}\left(\frac{Q}{n_i qAL \tanh\frac{W}{2L}}\right)^2, \tag{18}$$

where primes are not used for the QS model, and C_{bcj} and W are given in terms of the instantaneous values of V_{bc} using (1).

If one were to assume that the QS approximation is valid for the IGBT, (17) and (18) would give the time rate of change of collector-base voltage and the time rate of change of base charge in terms of the instantaneous values of I_T, V_{bc}, and Q. In effect, it is assumed in the QS approach that the changing base width can be accounted for by substituting the instantaneous value of base width into the expression for the collector current that was derived

for a constant base width, thereby neglecting any effect that the changing base width may have on the form of this expression for collector current. In addition, it is assumed in the QS approach that the interaction between the transport of electrons and holes is the same, as if the base current for corresponding steady-state conditions were flowing through the base. In fact, the base current supplied by the MOSFET is removed at the onset of the transient. It is also assumed in the QS approach that the shape of the excess carrier distribution is the same, as if recombination in the base were supplied by base current just as for the steady-state condition. In fact, recombination in the base is supplied by a reduction in the local excess carrier concentration during the transient.

Non-Quasi-Static State Equations

The NQS voltage state equation is obtained by substituting the NQS collector current given by (13) into the right-hand side of (15), expressing dW/dt in terms of dV_{bc}/dt using (5c), and by then combining the terms containing dV_{nc}/dt and those containing I_T. The NQS charge state equation is obtained by substituting the NQS expression for P_0 in terms of Q obtained from (12) into (16). The resulting NQS state equations are given by

$$\frac{dV_{bc}'}{dt} = \frac{I_T' - \dfrac{4D_p}{W'^2} Q'}{C_{bcj}'\left(1 + \dfrac{1}{b}\right)\left[1 + \dfrac{Q'}{3qAN_BW'}\right]}, \quad (19)$$

$$\frac{dQ'}{dt} = -\frac{Q'}{\tau_{HL}} - \frac{4Q'^2I_{sne}}{W'^2A^2q^2n_i^2}, \quad (20)$$

where C_{bc_j} and W are given in terms of the instantaneous values of V_{bc} using (1).

The denominator of (19) can be viewed as an effective output capacitance. The last term in the brackets in the denominator is a result of the moving boundary redistribution component of collector current and is equal to one-third times the ratio of the total excess carrier base charge Q to the background mobile carrier charge of the undepleted base ($qAN_B W$). This term appears as a capacitance because the moving boundary redistribution current is proportional to dV_{bc}/dt just as is the depletion-capacitance displacement current. Because most of the base is in the high-level injection condition, this term is large compared to unity (the first term in the brackets in the denominator), and the moving boundary redistribution current dominates the effective output capacitance and thus the voltage rate of rise. However, for a low-level injection condition, this term is less than unity, and the depletion capacitance dominates as in the QS voltage state equation. Also, for a high gain and typical loading conditions, the numerator of (19) approaches zero and the moving boundary component of current is not a significant component of the total current. Therefore, the NQS moving boundary redistribution effect is only important for the low-gain, high-level injection conditions of con-

ductivity-modulated devices. As previously stated, the coupling between the transport of electrons and holes is also only important for the low-gain, high-level injection conditions.

V. COMPARISON OF QS AND NQS MODELS

In this section, examples are presented that compare the predictions of the QS and NQS models with experimental results. To examine separately each of the two NQS effects mentioned above, both constant current and constant voltage conditions are studied. The predictions of the QS and NQS models are also compared with experimental current and voltage waveforms for the series resistor-inductor load. The comparisons are performed for devices with the parameters listed in Table I and for various device base lifetimes (an exception to Table I is that the base width for 0.3-μs device is 110 μm). It was shown in [6] and [7] that the NQS model can be used to describe consistently the steady-state and transient characteristics of IGBT's with different base lifetimes, and in reference [8] it was shown that the NQS IGBT state equations can be used to describe device-circuit interactions. In this section, it is shown that QS models cannot accurately describe the transient current and voltage waveforms so that the NQS approach is essential.

Constant Anode Voltage Switching

First, consider the turn-off current waveform for the anode voltage held constant by a large-valued, low-inductance capacitor at the anode of the device where the steady-state current is determined by the magnitude of the gate voltage pulse. The turn-off current waveform for this condition consists of an initial rapid fall in current followed by a slowly decaying portion. This is shown in Fig. 6 where the steady-state current before the device is switched off is defined as $I_T(0^-)$, and the initial value of the slowly decaying portion immediately after the devices is switched off is defined as $I_T(0^+)$. The initial rapid fall in current results from the removal of the MOSFET current and from the associated reduction in collector current due to the coupling between the transport of electrons and holes. This reduction in collector current is accounted for in the NQS model by the first term on the right-hand side of (13), but it is assumed in the QS model that this component of collector current is the same as if the steady-state base current continued to flow through the base. The last term on the right-hand side of (13) is zero for the constant anode voltage condition, so the moving boundary redistribution effect is unimportant for this loading condition.

For the QS model, $I_T(0^+)$ is assumed to be equal to the steady-state collector current given by (10); but for the NQS model, $I_T(0^+)$ is obtained by substituting the steady-state charge given by (7) into (13) where $I_T = I_p(W)$. The predicted and measured values of the relative size of the slowly decaying portion of the current waveform, $I_T(0^+)/I_T(0^-)$, are shown as a function of base liftetime in Fig. 7 for $I_T(0^-) = 5$ A and 0.25 A. The

TABLE I
DEVICE MODEL PARAMETERS

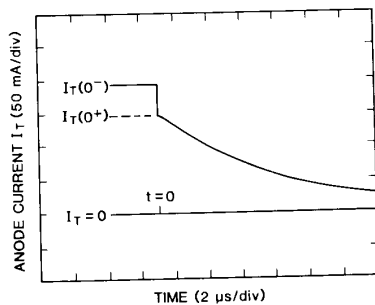|	
n_i	1.45×10^{10} cm^{-3}
μ_n	1500 cm^2/V-s
μ_p	450 cm^2/V-s
ϵ_{si}	1.05×10^{-12} F/cm
v_{psat}	10^7 cm/s
N_B	2×10^{14} cm^{-3}
A	0.1 cm^2
W_B	93 μm
I_{sne}	6.0×10^{-14} A

Fig. 6. Switching transient current waveform for IGBT being switched off, indicating current immediately before $I_T(0^-)$ and immediately after $I_T(0^+)$ initial rapid fall in current.
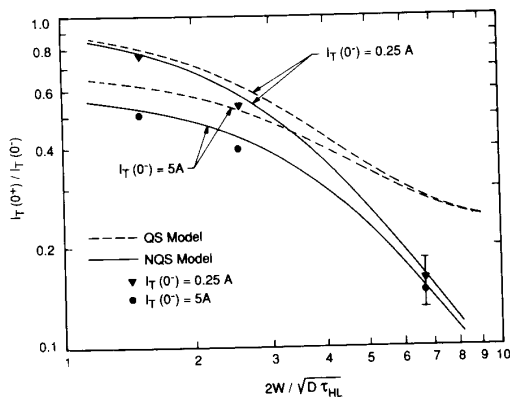

Fig. 7. Comparison of QS and NQS model results with measured values of $I_T(0^+)$ versus base lifetime for constant voltage switching.

predictions of the QS model are indicated by the dashed curves and the predictions of the NQS model are indicated by the solid curves. The QS model leads to the conclusion that the relative size of the slowly decaying portion of the turn-off current waveform is equivalent to the steady-state common base current gain of the bipolar transistor. Comparisons between the steady-state current gain and the relative size of the slowly decaying portion of the current waveform are made in [9] and [17]. However, it is evident from Fig. 7 that there is a significant difference between the predictions of the QS and NQS models when the gain is low, so the NQS model must be used to describe accurately the relative size of the slowly decaying portion of the current waveform [5]-[8]. In Fig. 7, the gain is low
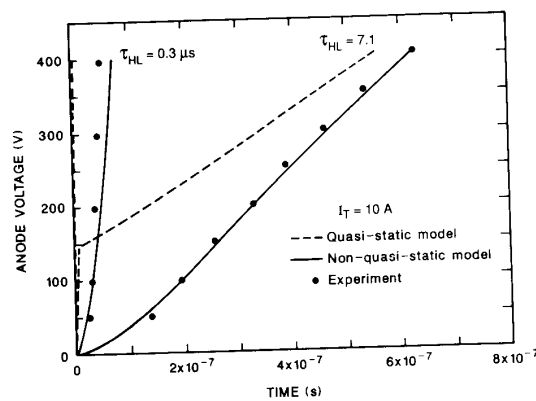

Fig. 8. Comparison of QS and NQS models with measured voltage waveforms for constant current switching and devices with different base lifetimes.

for the 5-A curve at the lowest values of $W/\sqrt{D\tau_{HL}}$ because of injection of electrons into the emitter, but for the remainder of the curves, the gain is determined by recombination in the base.

Constant Anode Current Switching

Next, consider the turn-off voltage waveform for the anode current held constant by a large inductor load (~ 1 mH) before the anode clamp voltage is reached. The measured and predicted anode voltage waveforms for this condition are shown in Fig. 8 for two different device base lifetimes, where the dashed curves are the predictions of the QS model and the solid curves are the predictions of the NQS model. The model predictions are obtained by simultaneously integrating the IGBT state equations ((17) and (18) for the QS model or (19) and (20) for the NQS model) using an automatic Runge–Kutta–Fehlberg method (RKF45 [18]), where the initial conditions of charge and voltage are obtained from the steady-state analysis.

The NQS voltage rate of rise for the curves of Fig. 8 is determined by the effective output capacitance (denominator of (19)), where the effective capacitive current supplies the difference between the total current and the charge-control collector current (numerator of (19)). For the high-level injection condition, the effective output capacitance is dominated by the moving boundary redistribution component of collector current which is accounted for in the NQS model by the second term in the brackets for in the NQS model by the second term in the brackets in the denominator of (19), but is not accounted for in the QS model. The voltage rate of rise varies by an order of magnitude between the different device base lifetimes of Fig. 8, because the effective output capacitance is proportional to the charge Q and the initial value of Q varies with the device base lifetime.

For the QS model, though, the initial voltage rate of rise is determined by the body-epitaxial layer depletion capacitance (denominator of (17)) as for a power MOSFET except that the collector current reduces the current that must be supplied by the displacement current (numerator of (17)). This initial QS voltage rate of rise of Fig. 8 is
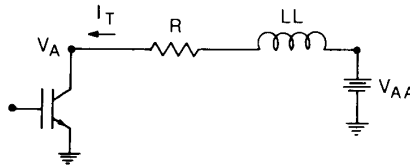
Fig. 9. Schematic of circuit used for modeling and measurement results shown in Figs. 10–12.
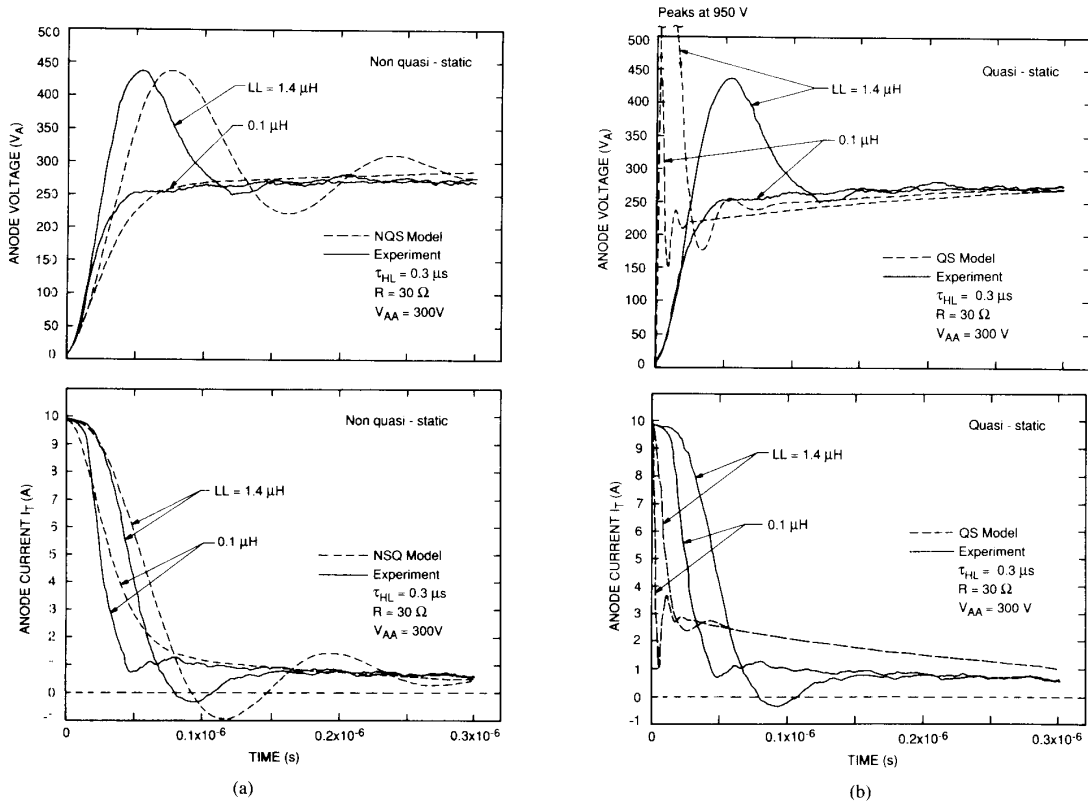

Fig. 10. Comparison of (a) NQS model and (b) QS model with measured turn-off current and voltage waveforms for 0.3-μs base lifetime device and inductances of 0.1 μH and 1.4 μH.

an order of magnitude faster than the measured voltage rate of rise for the 0.3-μs device, and is two orders of magnitude faster than the measured voltage rate of rise for the 7.1-μs device. For the 7.1-μs device, the base width is reduced during the QS voltage rise to the point where the numerator of (17) becomes zero. Beyond this point (e.g., 150 V for the 7.1-μs device in Fig. 8), the QS voltage rate of rise is determined by the rate of decay of charge, i.e., W decreases so that the numerator of (17) remains nearly equal to zero as Q decreases. This results in the two-phase QS voltage waveform of the 7.1-μs device in Fig. 8.

Series Resistor-Inductor Load Switching

Finally, consider the turn-off current and voltage waveforms for the series resistor-inductor load circuit shown

in Fig. 9. The state equation for this load circuit is given by

$$\frac{dI_T'}{dt} = \frac{1}{LL} \left(V_{AA} - I_T' R - V_A' \right) \tag{21}$$

where V_A is approximately equal to V_{bc} for the high-voltage transients discussed in this paper. To obtain the current and voltage turn-off switching waveforms, (21) is integrated simultaneously with the state equations of the IGBT ((17) and (18) for the QS model or (19) and (20) for the NQS model) using an automatic Runge–Kutta–Fehlberg method (RKF45 [18]), where the initial conditions are obtained from the steady-state analysis. Figs. 10–12 compare the predictions of the QS model and the NQS model with measured series resistor-inductor load turn-off waveforms for $V_{AA} = 300$ V, $R = 30$ Ω, and for different values of inductance. Each figure is for a differ-
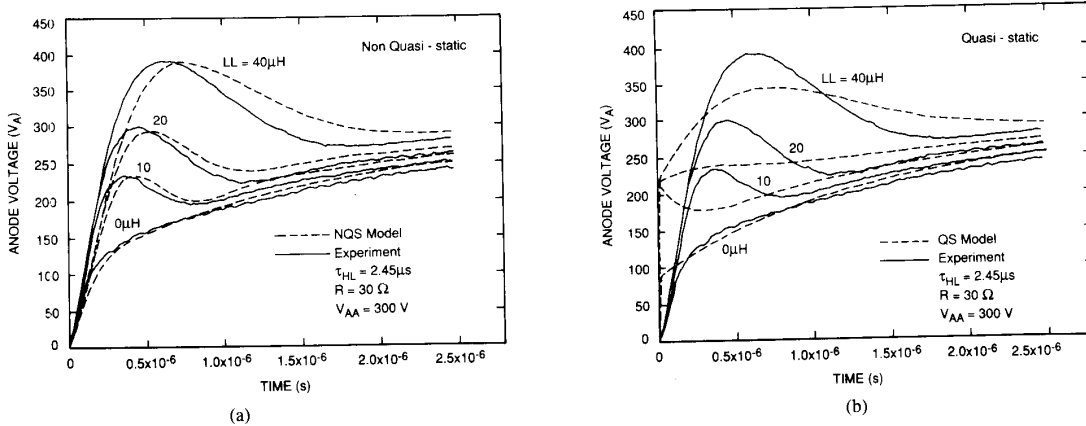
Fig. 11. Comparison of (a) NQS model and (b) QS model with measured turn-off voltage waveforms for 2.45-μs base lifetime device and inductances from 0 μH to 40 μH.
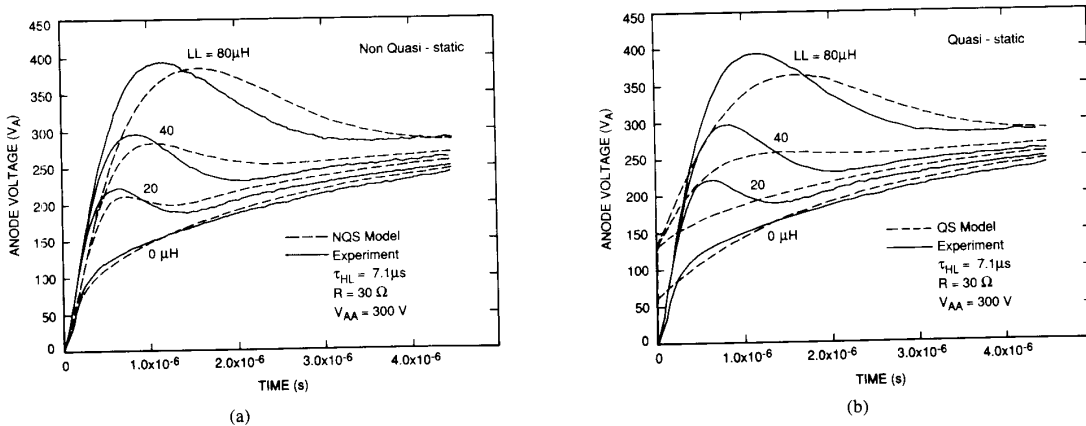

Fig. 12. Comparison of (a) NQS model and (b) QS model with measured turn-off voltage waveforms for a 7.1-μs base lifetime device and inductances from 0 μH to 80 μH.

ent device base lifetime, 0.3 μs, 2.45 μs, and 7.1 μs for Figs. 10, 11, and 12, respectively.

The predictions of the NQS model shown in Figs. 10(a), 11(a), and 12(a) are in qualitative agreement with the measured voltage waveforms and adequately describe the voltage overshoot for a given inductance. However, the initial voltage rate of rise predicted by the QS model (Figs. 10(b), 11(b), and 12(b)) is orders of magnitude larger than for the measured voltage waveforms. This occurs because the moving boundary redistribution effect on the output capacitance is not accounted for in the QS model. The voltage overshoot is overestimated by the QS model for the 0.3-μs device of Fig. 10(b) because the effective output capacitance is lower. But for the 2.45-μs and 7.1-μs devices of Figs. 11(b) and 12(b), the voltage overshoot is underestimated by the QS model because the voltage across the inductor initially rises to a larger value and the energy in the inductor is reduced more rapidly for the initial part of the two-phase voltage waveform. In general, the IGBT device-circuit interactions cannot be described using the QS approach, but the NQS effects become less important for devices with larger bipolar transistor current

gains; e.g., the QS voltage waveforms for the 7.1-μs device of Fig. 12(b) approach the measured waveforms more closely than those for the lower lifetime (lower gain) devices.

The NQS current waveforms shown in Fig. 10(a) for the 0.3-μs device are in qualitative agreement with the measured waveforms and accurately predict the initial value of the slowly decaying portion of the waveform. However, the slowly decaying portions of the QS current waveforms shown in Fig. 10(b) are larger than those of the measured waveforms because the coupling between the transport of electrons and holes is assumed to be the same as for the corresponding steady-state conditions. The initial fall in current is also more rapid for the QS model than for the measured waveforms because the voltage across the inductor is larger for the more rapid anode voltage rate of rise. The current waveforms for the 2.45-μs and 7.1-μs devices are not shown because they do not differ substantially between the QS and NQS models; the NQS current waveforms for these same conditions are presented in [8]. The slowly decaying portions do not differ between the predictions of the QS and NQS models

for the 2.45-μs and 7.1-μs devices because the current gain of these devices is high for the reduced value of W at 300 V.

VI. CONCLUSION

The QS approximation is not valid for the IGBT, and QS models cannot accurately describe the transient current and voltage waveforms of the IGBT. This is so because the QS approximation does not properly account for the change in the component of collector current due to the coupling between the transport of electrons and holes, nor does it account for the several-order-of-magnitude increase in effective output capacitance due to the rapidly changing quasi-neutral base width. The NQS model does, however, include these effects and can accurately describe the transient current and voltage waveforms of the IGBT for general loading conditions. These effects dominate transient operation for the low-gain, high-level injection conditions of the IGBT, but are unimportant for the high-gain or low-level injection conditions of signal transistors.

NOMENCLATURE†

A	Device active area (cm^2).
I_n, I_p	Electron, hole current (A).
I_T	Anode current (A).
I_{sne}	Emitter electron saturation current (A).
n, p	Electron, hole carrier concentration (cm^{-3}).
$\delta n, \delta p$	Excess carrier concentration (cm^{-3}).
P_0	δp at $x = 0$ (cm^{-3}).
n_i	Intrinsic carrier concentration (cm^{-3}).
Q	Total excess carrier base charge (C).
ϵ_{si}	Dielectric constant of silicon (F/cm).
q	Electronic charge (1.6×10^{-19} C).
μ_n, μ_p	Electron, hole mobility (cm^2/V-s).
D_n, D_p	Electron, hole diffusivity (cm^2/s).
τ_{HL}	Base high-level lifetime (s).
$b \equiv \mu_n / \mu_p$	Ambipolar mobility ratio.
$D \equiv 2D_n D_p / D_n + D_p$	Ambipolar diffusivity (cm^2/s).
$L \equiv \sqrt{D\tau_{HL}}$	Ambipolar diffusion length (cm).
x	Distance in base from emitter (cm).
W_B	Metallurgical base width (cm).
W	Quasi-neutral base width (cm).
W_{bcj}	Collector-base depletion width (cm).
$C_{bcj} \equiv A\epsilon_{si} / W_{bcj}$	Collector-base depletion capacitance (F).
N_B	Base doping concentration (cm^{-3}).
V_{bi}	Built-in junction potential (V).
V_{bc}	Applied collector-base voltage (V).
V_A	Device anode voltage (V).
V_{AA}	Anode supply voltage (V).
LL	Series load inductance (H).
R	Series load resistance (Ω).
$\tau_b \equiv W^2 / 4D_p$	High-gain, high-level injection base transit time (s).

†Parameters that change with time are distinguished with a prime for the NQS transient analysis.

REFERENCES

[1] J. P. Russell, A. M. Goodman, L. A. Goodman, and J. M. Neilson, "The COMFET—A new high conductance MOS-gated device," *IEEE Electron Devices Lett.*, vol. EDL-4, p. 63, 1983.

[2] B. J. Baliga, M. S. Adler, R. P. Love, P. V. Gray, and N. D. Zommer, "The insulated gate transistor: A new three-terminal MOS-controlled bipolar power device," *IEEE Trans. Electron Dev.*, vol. ED-31, p. 821, 1984.

[3] H. Yilmaz, W. R. Van Dell, K. Owyang, and M. F. Chang, "Insulated gate transistor modeling and optimization," in *Tech. Dig. IEEE Intern. Elec. Dev. Meet.*, p. 274, 1984.

[4] A. R. Hefner and D. L. Blackburn, "Performance trade-off for the insulated gate bipolar transistor: buffer layer versus base lifetime reduction," *IEEE Trans. Power Electron.*, vol. PE-2, p. 194, 1987; also in *Conf. Rec. IEEE Power Elec. Spec. Conf.*, 1986, vol. 27.

[5] A. R. Hefner, D. L. Blackburn, and K. F. Galloway, "The effect of neutrons on the characteristics of the insulated gate bipolar transistor (IGBT)," *IEEE Trans. Nucl. Sci.*, vol. NS-33, p. 1428, 1986.

[6] A. R. Hefner, "Characterization and modeling of the power insulated gate bipolar transistor," Ph.D. dissertation, University of Maryland, College Park, Ann Arbor, MI: *University Microfilms International*, 1987.

[7] A. R. Hefner and D. L. Blackburn, "An analytical model for the steady-state and transient characteristics of the power insulated gate bipolar transistor," *Solid-State Electronics*, vol. 31, p. 1513, 1988.

[8] A. R. Hefner, "Analytical modeling of device-circuit interactions for the power insulated gate bipolar transistor (IGBT)," in *Conf. Rec. IEEE Ind. Appl. Soc. Meet.*, 1988, p. 606. Also scheduled for publication in *IEEE Trans. Ind. Appl.*, vol. 26, no. 6, Nov. 1990.

[9] D.-S. Kuo and C. Hu, "An analytical model for the power bipolar-MOS transistor," *Solid-State Electronics*, vol. 29, p. 1229, 1986.

[10] J. G. Fossum and R. J. McDonald, "Charge-control analysis of the COMFET turn-off transient," *IEEE Trans. Electron Devices*, vol. ED-33, p. 1377, 1986.

[11] J. G. Fossum, R. J. McDonald, and M. A. Shibib, "Network representations of LIGBT structures for CAD of power integrated circuits," *IEEE Trans. Electron Devices*, vol. ED-35, p. 507, 1988.

[12] J. G. Fossum and Y.-S. Kim, "Static and dynamic latchup in the LIGBT," *IEEE Trans. Electron Devices*, vol. ED-35, 1977, 1988.

[13] A. S. Grove, *Physics and Technology of Semiconductor Devices*. New York: Wiley, 1967, p. 222.

[14] M.-K. Chen, F. A. Lindholm, and B. S. Wu, "Comparison and extension of recent one-dimensional transistor models," *IEEE Trans. Electron Dev.*, vol. ED-35, p. 1096, 1988.

[15] W. van Roosbroeck, "The Transport of Added Current Carriers in a Homogeneous Semiconductor," *Physical Review*, vol. 91, p. 282, 1953.

[16] E. Stein and D. Schroder, "Computer aided design of circuits for power controlling with the new power elements MOSFET and SIT," in *Conf. Rec. IEEE Ind. Appl. Soc. Meet.*, 1984, p. 766.

[17] B. J. Baliga, "Analysis of insulated gate bipolar transistor turn-off characteristics," *IEEE Electron Dev. Lett.*, vol. EDL-6, p. 74, 1985.

[18] G. E. Forsythe, M. A. Malcolm, and C. B. Moler, *Computer Methods for Mathematical Computations*. Englewood Cliffs, NJ: Prentice-Hall, 1977, p. 129.

Allen R. Hefner, Jr. (S'84-M'84-S'85-S'86-M'86-M'87) was born in Washington DC on June 29, 1959. He received the B.S., M.S., and Ph.D. degrees in electrical engineering from the University of Maryland, College Park, in 1983, 1985, and 1987 respectively.

He joined the Semiconductor Electronics division of the National Institute of Standards and Technology (formerly the National Bureau of Standards) in 1983, where he has been working in the device technology area.

Dr. Hefner's research interests include characterization, modeling, and circuit utilization of power semiconductor devices. He is the author of several technical publications and has presented several talks at technical meetings describing research on the Insulated Gate Bipolar Transistor. He is currently a member of the Working Group on Device Models within the IEEE Power Electronics Society Technical Committee for Computers in Power Electronics, and is the Transactions Paper Review Chairman for the Power Semiconductor Committee of the IEEE Industry Applications Society.